



HAL
open science

Frustrated behavior of Lewis/Brønsted pairs inside molecular cages

Chunyang Li, Anne-Doriane Manick, J-P Dutasta, X Bugaut, B Chatelet, Alexandre Martinez

► **To cite this version:**

Chunyang Li, Anne-Doriane Manick, J-P Dutasta, X Bugaut, B Chatelet, et al.. Frustrated behavior of Lewis/Brønsted pairs inside molecular cages. *Organic Chemistry Frontiers*, 2022, 9, pp.1826 - 1836. 10.1039/d2qo00011c . hal-03961770

HAL Id: hal-03961770

<https://hal.science/hal-03961770>

Submitted on 7 Feb 2023

HAL is a multi-disciplinary open access archive for the deposit and dissemination of scientific research documents, whether they are published or not. The documents may come from teaching and research institutions in France or abroad, or from public or private research centers.

L'archive ouverte pluridisciplinaire **HAL**, est destinée au dépôt et à la diffusion de documents scientifiques de niveau recherche, publiés ou non, émanant des établissements d'enseignement et de recherche français ou étrangers, des laboratoires publics ou privés.

Frustrated behavior of Lewis/Brønsted pairs inside molecular cages†

C. Li,^{a,b} A.-D. Manick,^b J.-P. Dutasta,^c X. Bugaut,^{b,d} B. Chatelet^{*b} and A. Martinez^{id}^{*b}

Different endohedrally functionalized cages were designed to investigate the effects of the size and shape of molecular cavities on the frustrated behavior of Lewis/Brønsted acid–base pairs and on catalytic activities. The shape of the inner space above the reactive center was found to strongly affect these properties. When an acidic azaphosphatrane is inserted in the smallest cage and associated with *t*-BuOK or ⁻CD₂CN bases, a frustrated Brønsted pair is obtained. In contrast, when encapsulated in the medium or large cage, the P–H⁺ azaphosphatrane acid is easily deprotonated under the same conditions. The resulting two supramolecular Verkade's superbases lead to frustrated Lewis pair systems in the presence of TiCl₄. Furthermore, the larger cage displays better catalytic activity in the MBH reaction. Thus, a small change in the cage size, which only differs by one methylene group in the linkers, can influence the frustrated properties of the related systems, and a right balance between the frustrated behavior and cage flexibility has to be reached to obtain optimal systems for catalytic applications.

Artificial cages have found a wide range of applications in guest binding,¹ transport,² gas adsorption,³ drug delivery,⁴ chemical purification,⁵ stabilization of reactive species⁶ and catalysis.⁷ Such complex structures have been obtained either by self-assembly or covalent strategies.^{8,9} When used as supramolecular catalysts, the nano-confinement of the reactants and/or the catalytic site can lead (i) to an increase in the reaction rate, for instance, by changing the conformation of the substrate or by stabilizing transition states,^{10–12} (ii) to an improvement or change in the selectivity by substrate size selectivity,¹³ by controlling the second coordination sphere or the folding of the substrate,^{14,15} or by masking with a supramolecular shadow some specific reactive sites,¹⁶ and (iii) to protection of the catalytic site, allowing for example the

improvement of the stability of the catalyst or sequential catalysis with incompatible systems.¹⁷

We recently reported that endohedral functionalization of the inner space of molecular cages can provide, in the presence of an acid, frustrated Lewis pairs (FLPs): the encapsulation of the Lewis base partner prevents its interaction with the Lewis acid, leading to FLPs active in catalysis (Scheme S1†).¹⁸ Indeed, the confined superbase, associated with titanium(IV) chloride as the Lewis acid, turns out to be an efficient catalyst for Morita–Baylis–Hillman (MBH) reactions, whereas the model superbase lacking a cavity exhibited no catalytic activity in MBH reactions, since these two partners interact and neutralize each other.¹⁸ Over the past few years, FLPs have aroused huge interest,¹⁹ for example for their ability to activate C–H or C–F bonds²⁰ and small molecules like H₂, N₂, or CO₂,²¹ and for their applications in new and original reactive systems for catalysis.²² Several strategies have been reported to modulate the FLP properties by changing either the electronic and steric properties of the units linked to the acid or Lewis sites,²³ or the nature of the Lewis acid or basic atoms.²⁴ Hence, new and original approaches, like “reverse FLP”, have emerged from these studies.²⁵ In this context, we decided to explore the frustrated behavior of Lewis/Brønsted pairs in the confined space of the inner cavity of covalent molecular receptors. This work describes the synthesis of Verkade's superbases,²⁶ encaged in three hemicryptophane hosts, differing only by one methylene group in each linker (Fig. 1). We demonstrate that this small structural change strongly alters their reactivity and their FLP behavior.

^aMaterial Corrosion and Protection Key Laboratory of Sichuan Province, Department of Materials and Chemistry Engineering, Sichuan University of Science and Engineering, Zigong, 643000, China

^bAix Marseille Univ., CNRS, Centrale Marseille, iSm2, Marseille, France.

E-mail: alexandre.martinez@centrale-marseille.fr,

bastien.chatelet@centrale-marseille.fr

^cLaboratoire de Chimie, École Normale Supérieure de Lyon, CNRS, 46, Allée d'Italie, F-69364 Lyon, France

^dUniversité de Strasbourg, Université de Haute-Alsace, CNRS, LIMA, UMR 7042, 67000 Strasbourg, France

†Electronic supplementary information (ESI) available. CCDC 2093016 and 2099451. For ESI and crystallographic data in CIF or other electronic format see DOI: 10.1039/d2qo00011c

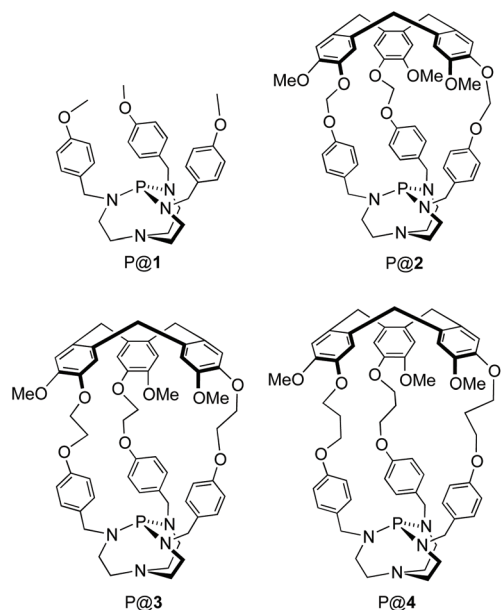


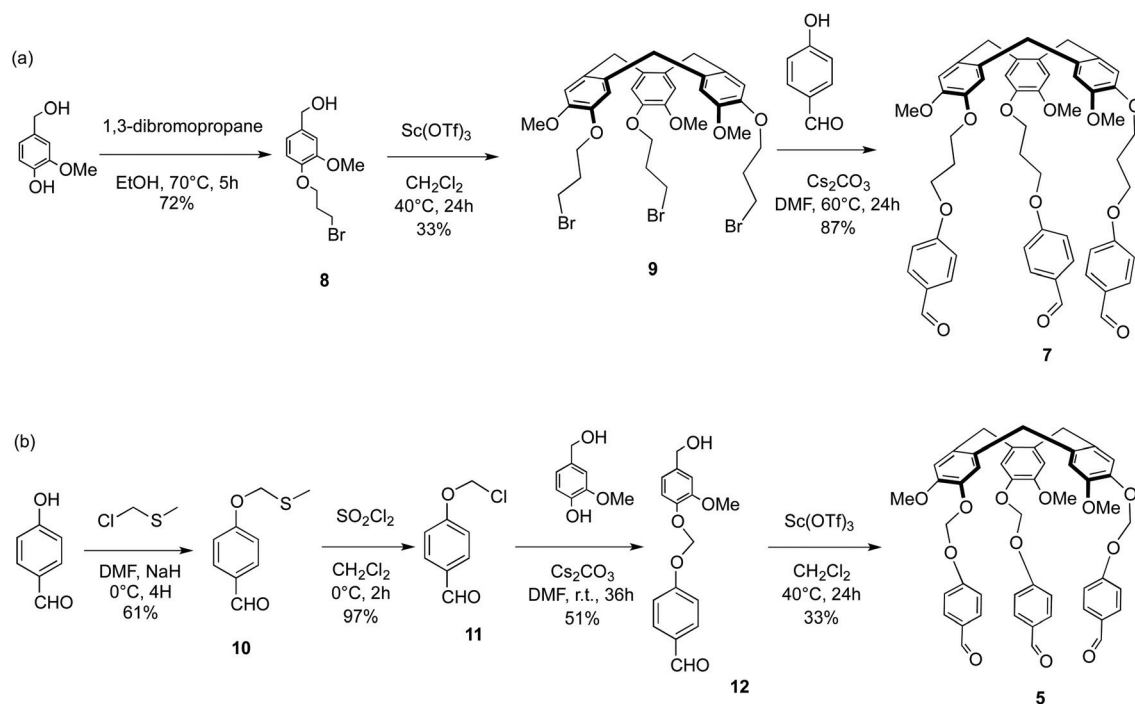
Fig. 1 Structures of the model and confined Verkade's superbases.

Results and discussion

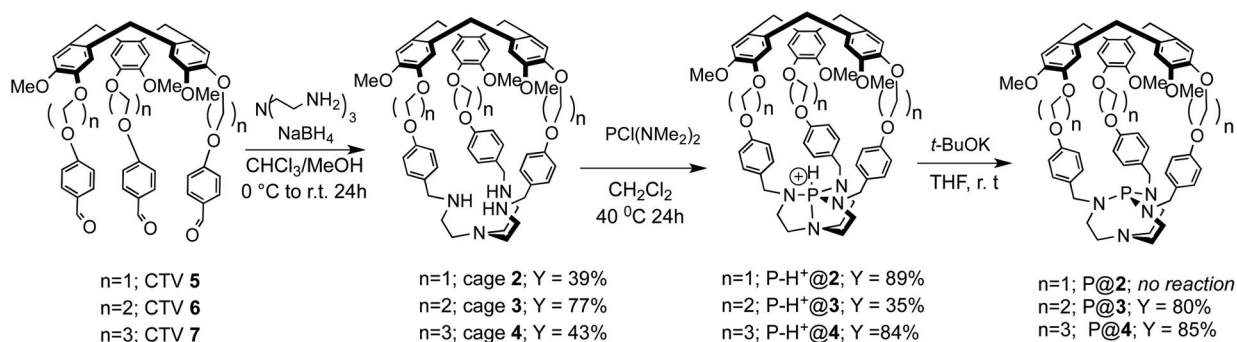
With the aim to finely tune the inner space of hemicryptophane cages, we synthesized Verkade's superbases P@2, P@3 and P@4 with respectively one, two and three methylene groups in the linkers, leading to small, medium and large cavity sizes (Fig. 1). We first prepared cyclotrimeratrylene (CTV)

derivatives 5, 6 and 7 (Schemes 1 and 2). CTV 6 was obtained according to the procedure reported previously.²⁷ A similar synthetic pathway was followed to isolate CTV 7 (Scheme 1(a)): mixing vanillyl alcohol and 1,3-dibromopropane provided compound 8 in 72% yield. The subsequent cyclisation step was performed in acetonitrile using scandium triflate as the Lewis acid and afforded the expected alkyl-brominated CTV 9 in 33% yield. The hemicryptophane precursor 7 was then obtained in 87% yield by reacting 9 with 4-hydroxybenzaldehyde in DMF in the presence of Cs₂CO₃. A slightly different strategy was used to synthesize CTV 5 (Scheme 1(b)) as the reactions of vanillyl alcohol with dichloromethane, dibromomethane, or chlorobromomethane led to the di-substituted derivative instead of the expected compound. Thus, *p*-hydroxybenzaldehyde reacted first with chloromethyl-methylsulfide in DMF at 0 °C for 4 h, affording 10 in 61% yield. In the next step, sulfonyl chloride was used as the chlorinating reagent to provide compound 11 in 97% yield. Then, the reaction of 11 with vanillyl alcohol in DMF using Cs₂CO₃ as a base afforded compound 12 in 51% yield. Finally, 12 was treated with scandium triflate in dichloromethane to give CTV 5 in 33% yield.

Hemicryptophane cages 2, 3 and 4 were obtained by the reaction of tris-(2-aminoethyl)amine (tren) with CTVs 5, 6 and 7, respectively, *via* a reductive amination using NaBH₄ (Scheme 2). The engaged azaphosphatranes P-H⁺@2, P-H⁺@3 and P-H⁺@4 were obtained by addition of PCl(NMe₂)₂ to a CH₂Cl₂ solution of 2, 3 and 4, respectively. The ¹H NMR spectra support that the C₃ symmetry is retained in solution (Fig. S9 and S30[†]),²⁸ and the ³¹P NMR spectra show characteristic signals at respectively -32, -32 and -23 ppm evidencing



Scheme 1 Synthetic pathways leading to CTVs 5 and 7.



Scheme 2 Synthetic pathway to obtain the encaged azaphosphatranes.

the formation of the azatrane structures (Fig. S11 and S33[†]).²⁸ Interestingly, when the reaction of **4** with $\text{PCI}(\text{NMe}_2)_2$ was performed in CH_3CN instead of CH_2Cl_2 , the expected $\text{P-H}^+\text{@4}$ was obtained in 18% yield, together with the amino-phosphine oxide **13** ($Y = 39\%$). The insertion of the phosphorus atom in the tren unit was probably not fully achieved at the hydrolysis step leading to the unexpected amino-phosphine **13**. Compound **13** was fully characterized by NMR spectroscopy, mass spectrometry (Fig. S16–S19[†]) and X-ray crystallography. The X-ray molecular structure shows a molecule of chloroform trapped inside the cavity of **13** and confirms the formation of the secondary phosphine oxide, linked to the cage by two nitrogen atoms (Fig. 2).

We then attempted to deprotonate the encaged azaphosphatranes in order to obtain the confined superbases P@2 , P@3 and P@4 , and to measure their $\text{p}K_a$ values. $\text{P-H}^+\text{@3}$ and $\text{P-H}^+\text{@4}$ were easily deprotonated with potassium *t*-butoxide in THF,²⁸ and NMR signals at +125 ppm and +115 ppm were respectively observed in the ³¹P NMR spectra, as expected for pro-azaphosphatrane derivatives (Fig. S15[†]).²⁸ The $\text{p}K_a$ value of P@4 was then estimated using our previous published procedure for P@3 : addition of $\text{P-H}^+\text{@4}$ to a solution in CD_3CN of the model Verkade's superbase P@1 allows for calculating the $\text{p}K_a$, from the ³¹P spectrum, once the thermodynamic equilibrium is reached (Fig. S41[†]).²⁸ A $\text{p}K_a$ value of 32.32 was found, lower than that of cage P@3 ($\text{p}K_a = 32.99$) and slightly higher than that of its model parent P@1 ($\text{p}K_a = 32.14$) (Table 1). The

Table 1 $\text{p}K_a$ values of conjugate acids of proazaphosphatrane bases in CH_3CN , and rate constants values for proton transfers^a

Base	$\text{p}K_a$	K_a	k_1 ($\text{L mol}^{-1} \text{s}^{-1}$)	k_{-1} ($\text{L mol}^{-1} \text{s}^{-1}$)
P@1 ²⁷	32.14	7.25×10^{-33}	1.06×10^{-3}	0.93×10^{-3}
P@2	— ^b	— ^b	— ^b	— ^b
P@3 ²⁷	32.99	1.03×10^{-33}	1.88×10^{-6}	1.16×10^{-5}
P@4	32.32	4.77×10^{-33}	1.04×10^{-6}	1.37×10^{-6}

^a Average values of at least two experiments, $T = 298$ K. Errors on the K_a , k_1 and k_{-1} values are estimated to 10%. ^b No reaction was observed.

greater flexibility of cage **4** could account for this less marked effect of the confinement on the basic properties of the encapsulated Verkade's superbase. Indeed, the higher basicity of P@3 , when compared to its related model P@1 , was attributed to the stabilization of its conjugated acid $\text{P-H}^+\text{@3}$ via cation- π interactions between the aromatic rings of the linkers and the cationic azaphosphatrane unit.²⁸ These interactions are probably less efficient with the larger and more flexible cage $\text{P-H}^+\text{@4}$. The rate of proton transfer was also measured (Table 1 and Scheme 3, eqn (1) and (2)).²⁸ As in the case of $\text{P-H}^+\text{@3}$, the deprotonation/protonation is much slower with $\text{P-H}^+\text{@4}$ than with its model counterpart $\text{P-H}^+\text{@1}$, proving that the cavity strongly affects the reaction rates.

However, the rate constants of deprotonation/protonation of P@3 and P@4 are in the same order of magnitude, supporting that the phosphorus atom is also not easily accessible in

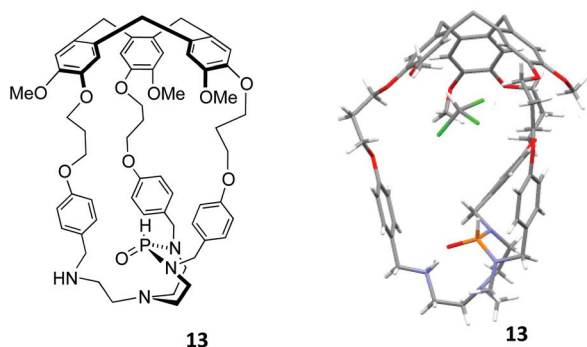
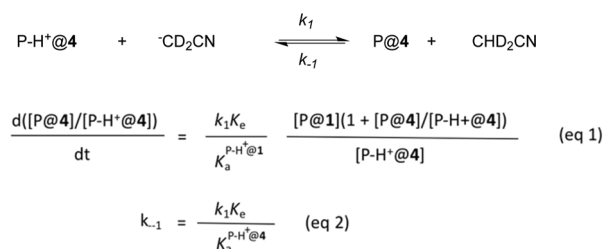


Fig. 2 X-ray molecular structure of hemicryptophane **13**.



Scheme 3 Acid–base equilibrium used for calculating proton transfer rates. Kinetics were monitored using ³¹P NMR to estimate at each time the concentration of the different species in eqn (1) and (2) and thus to calculate k_1 and k_{-1} (see ESI[†] for more details).

P@4 despite the larger cavity size. This suggests that an FLP system could also be obtained with P@4 once associated with a Lewis acid as previously observed for the P@3/TiCl₄ system.

The same set of experiments was then carried out with P-H⁺@2. No reaction occurred when potassium *t*-butoxide is mixed with P-H⁺@2 in THF. When increasing the number of equivalents of potassium *t*-butoxide or the temperature, the reaction medium remains unchanged. We hypothesized that potassium *t*-butoxide is too big to fit inside this small cavity, and we decided to perform the deprotonation using the smaller and planar ⁻CD₂CN anion. Thus, P-H⁺@2 was solubilized with the model compound P@1 in CD₃CN in an NMR sealed tube, and the reaction mixture was left standing for several weeks, but no reaction took place even after heating for days. Other attempts using small base-like methanolate or NaH also failed to provide the expected pro-azaphosphatrane. Thus, a slight decrease of the cavity size achieved by removing only one methylene group in each linker prevents the acid-base reaction, leading to frustrated Brønsted pairs P-H⁺@2/*t*-BuOK and P-H⁺@2/⁻CD₂CN. This highlights how a minor change in the size of the cavity can strongly affect the reactivity of the engaged Brønsted base. Crystals of P-H⁺@2 suitable for X-ray diffraction were obtained by slow diffusion of ether in a solution of P-H⁺@2 in chloroform. The X-ray structure reveals a narrow cavity above the azaphosphatrane unit without any solvent molecule trapped inside (Fig. 3). This suggests that the cavity is too small to accommodate even a small molecule of the solvent. Moreover, the aromatic rings of the linkers adopt a helical arrangement: the chirality of the CTV propagates along the linkers and the lateral arms present a Λ (respectively Δ) propeller-like arrangement that is imposed by the *M* configuration (respectively *P*) of the CTV unit.²⁹ This induces a strong twist of the whole framework leading to extremely narrow windows and probably precluding the access of a basic molecule to the azaphosphatrane center. This could account for the lack of reaction between the acidic azaphosphatrane unit and the basic ⁻CD₂CN, MeO⁻, NaH or *t*-BuO⁻.

We then compared the ability of P@3 and P@4 to behave as FLP systems. To that end, the catalytic properties of the FLP systems P@3/TiCl₄ and P@4/TiCl₄ in the Morita-Baylis-Hillman (MBH) reactions between cycloenone and benz-

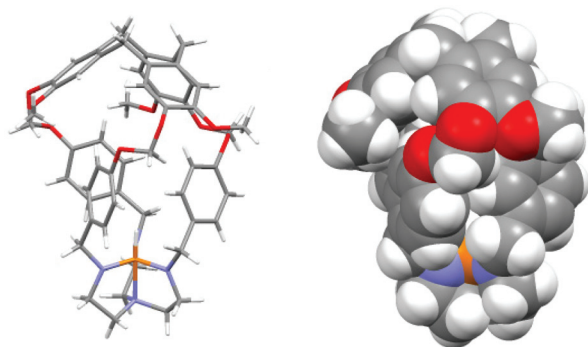


Fig. 3 X-ray molecular structure of P-H⁺@2.

aldehyde derivatives were investigated. We have previously demonstrated that very low yields are obtained with the model P@1/TiCl₄ system. Indeed, an interaction followed by a reaction between the two Lewis acid/base partners led to the formation of a chloroazaphosphatrane devoid of any catalytic activity.¹⁸

This reaction is prevented with the P@3/TiCl₄ system, allowing for the restoration of the catalytic activities. We wondered if the larger cavity in P@4 could allow interactions with the Lewis acid TiCl₄ resulting in the formation of an engaged chloroazaphosphatrane P-Cl@4, and leading to a decrease in catalytic activity. We thus decided to use this reaction as a model to test if the pair P@4/TiCl₄ also behaves as an FLP system. In Fig. 4 we report the results obtained with the P@1/TiCl₄, P@3/TiCl₄ and P@4/TiCl₄ systems.

The P@4/TiCl₄ pair presents a catalytic activity much higher than that of the P@1/TiCl₄ system, and similar or better than that obtained with the P@3/TiCl₄ one. As shown in Fig. 4(a), when cyclopentenone is used as the substrate, P@3/TiCl₄ and P@4/TiCl₄ catalytic systems give similar yields using *p*-chloro-benzaldehyde (75% and 74%, respectively) or *p*-nitro-benzaldehyde (55% for both systems) as reactants. With *p*-methyl-benzaldehyde as the electrophile, yields of 44% and 51% were achieved with P@3/TiCl₄ and P@4/TiCl₄, respectively. Better catalytic activity of the P@4/TiCl₄ pair compared to the P@3/TiCl₄ one is also observed when cyclohexenone is used as the substrate (Fig. 4(b)). Higher yields are obtained with the previous system whatever the aldehyde used. Yields of 71%, 66% and 86% are achieved with the P@4/TiCl₄ pair and *p*-chloro-, *p*-methyl-, or *p*-nitro-benzaldehyde as electrophiles, respectively, compared with 63%, 48% and 81% yields respectively obtained with P@3/TiCl₄ as the catalytic system for the same set of reactions. The larger size of the cavity of P@4 compared to that of P@3, probably allows better adaptation of

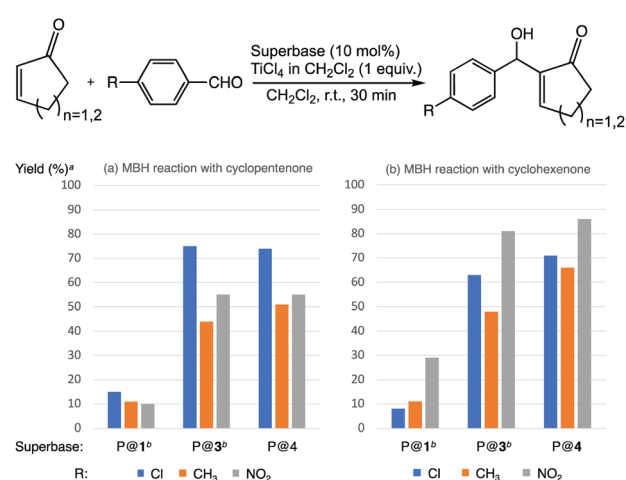


Fig. 4 The Morita Baylis Hillman reaction catalyzed by different systems. Reaction conditions: aldehyde (0.3 mmol), enone (0.9 mmol), catalyst (0.03 mmol, 10 mol%), TiCl₄ (1 M in CH₂Cl₂, 0.3 mmol), CH₂Cl₂ (1.0 mL), 30 min under argon atmosphere. ^a Isolated yields (average of at least two runs). ^b From ref. 18.

larger reaction intermediates or transition states, which explains the better activity of the P@4/TiCl₄ system when cyclohexenone is used as a substrate. The ³¹P NMR spectra of the crude reaction mixtures of the MBH reactions confirm that no formation of the chloroazaphosphatane P-Cl⁺@4 occurs during the reaction (Fig. S40[†]). This demonstrates that the interaction between the Lewis base P@4 and the Lewis acid TiCl₄ is still prevented despite the larger cavity of P@4, and that P@4/TiCl₄ constitutes an FLP system. This latter system appears more efficient than P@3/TiCl₄ in this MBH reaction, probably because it presents the right balance between (i) flexibility to accommodate substrates and transition states more easily and (ii) the frustrated behavior to prevent Lewis acid-base interaction.

Conclusion

In conclusion, the ability of endohedrally functionalized cages to control the frustration level of acid/base couples has been studied. The simple change of one methylene group in the linkers of the cages allows for controlling the reactivity of the encaged basic unit. Indeed, the smaller cage leads to an extremely frustrated system that even prevents its deprotonation, giving the fully frustrated Brønsted pairs P-H⁺@2/*t*-BuOK and P-H⁺@2/⁻CD₂CN. In contrast, the medium and large cages can be easily deprotonated under the same conditions. In the presence of the TiCl₄ Lewis acid, the medium P@3 and large P@4 cages lead to FLPs. Nevertheless, the P@4/TiCl₄ system can provide better yields in the MBH reaction when cyclohexanone is used as the substrate, underlining that if rigidity is key to preventing the Lewis acid/base interaction, some flexibility has to be retained to induce an improvement of the reactivity. Thus, the confinement in well-defined molecular cages appears as an efficient tool to control the degree of frustration of the acid and the base, opening the way to a wider use of this strategy to modulate FLP systems.

Experimental section

Commercial reagents were used directly as received without further purification. All reactions were performed in oven-dried glassware under positive pressure of argon, unless otherwise noted. Fritted glass were subsequently neutralized with saturated NaHCO₃ solution, twice rinsed with distilled water and acetone, and then oven-dried. Dichloromethane, tetrahydrofuran and toluene were dried prior to use through standard procedures or obtained from a solvent drying system BRAUN MB-SPS800. ¹H and ¹³C NMR spectra were recorded on a Bruker AC 400 (400 MHz for ¹H NMR, 101 MHz for ¹³C NMR, and 162 MHz for ³¹P NMR in CDCl₃ or CD₂Cl₂). Chemical shifts were reported in ppm on the δ scale relative to residual CDCl₃ (δ = 7.26 for ¹H NMR and δ = 77.16 for ¹³C NMR) and CD₂Cl₂ (δ = 5.32 for ¹H NMR and 53.84 for ¹³C NMR) as the internal references. The coupling constant (*J*) is reported in

hertz (Hz). Multiplicities are described with the following standard abbreviations: s = singlet, br = broad, d = doublet, t = triplet, q = quadruplet, m = multiplet. Column chromatography was performed with gel 60 (Macherey-Nagel® Si 60, 0.040–0.063 mm). Analytical thin layer chromatography (TLC) was carried out on Merck®Kieselgel 60 F254 plates and under a 254 nm UV lamp. High-resolution mass spectra (HRMS) were obtained on a SYNAPT G2 HDMS (Waters) spectrometer equipped with an atmospheric pressure ionization source (API) pneumatically assisted. Compound **10** and hemicryptophanes **3**, PH⁺@3 and P@3 were synthesized according to previous reported procedures.^{28,30}

Compound 8

In a dried round-bottomed flask, vanillyl alcohol (10 g, 64.86 mmol) and potassium carbonate (10 g, 72.36 mmol) were dissolved in ethanol (500 mL), and 1,3-dibromopropane (16.45 mL, 162.08 mmol) was added drop-wise. The mixture was vigorously stirred and heated at 70 °C for 5 h. The solvent was removed under reduced pressure, and the crude residue was dissolved in CH₂Cl₂ (200 mL) and washed with 1 M NaOH solution (200 mL × 3). After 2 h, the precipitate that formed was filtered through fritted glass, and the organic phase was dried over anhydrous Na₂SO₄ and concentrated *in vacuo* to give a brown oil. The crude compound was purified by silica gel column chromatography using CH₂Cl₂ as the eluent to give pure **8** as a white solid (12.85 g, 72%). *T*_m: 61–62 °C. IR: cm⁻¹ 3332, 2935, 2867, 2184, 1743, 1591, 1511, 1463, 1418, 1384, 1357, 1324, 1258, 1229, 1155, 1134, 1102, 1076, 1059, 1026, 915, 891, 653, 799, 761, 718, 761, 718, 646, 550. HRMS (ESI): *m/z* [M + Na]⁺ calcd for C₁₁H₁₅BrO₃, 297.0097; found at 297.0094; ¹H NMR (400 MHz, CDCl₃) δ = 6.92 (d, *J* = 1.7 Hz, 1H), 6.89–6.84 (m, 2H), 4.60 (d, *J* = 3.0 Hz, 2H), 4.14 (t, *J* = 6.0 Hz, 2H), 3.85 (s, 3H), 3.62 (t, *J* = 6.5 Hz, 2H), 2.35 (quintuplet, *J* = 6.2 Hz, 2H), 1.82 (t, *J* = 10.9 Hz, 1H); ¹³C NMR (101 MHz, CDCl₃) δ = 149.9, 147.9, 134.5, 119.6, 113.9, 111.2, 67.1, 65.3, 56.1, 32.5, 30.2.

Compound 9

In a dried round-bottomed flask, **8** (5 g, 18.17 mmol) was dissolved in acetonitrile (100 mL), and a catalytic amount of scandium III triflate (447 mg, 9.09 mmol) was added. The mixture was vigorously stirred and heated at 80 °C for 36 h. The solvent was removed under reduced pressure, and the crude residue was dissolved in CH₂Cl₂ (150 mL) and washed with 1 M NaOH solution (150 mL × 3). The organic phase was dried over anhydrous Na₂SO₄ and CH₂Cl₂ was concentrated *in vacuo* to give a brown oil. The crude compound was purified by silica gel column chromatography using CH₂Cl₂ as the eluent to give pure **9** as a white solid (1.54 g, 33%). *T*_m: 132–133 °C. IR: cm⁻¹ 2930, 2871, 1607, 1511, 1466, 1398, 1320, 1262, 1220, 1194, 1089, 1029, 943, 876, 852, 743, 622, 570. HRMS (ESI): *m/z* [M + Na]⁺ calcd for C₃₃H₃₉Br₃O₆, 795.0154; found at 795.0153; ¹H NMR (300 MHz, CDCl₃) δ = 6.91 (s, 3H), 6.85 (s, 3H), 4.76 (d, *J* = 13.7 Hz, 3H), 4.13 (td, *J* = 6.0, 1.3 Hz, 6H), 3.83 (s, 9H), 3.60 (td, *J* = 6.6, 2.5 Hz, 6H), 3.53 (d, *J* = 13.8 Hz, 3H), 2.33 (quintu-

plet, $J = 6.1$ Hz, 6H); ^{13}C NMR (75 MHz, CDCl_3) $\delta = 148.6, 147.0, 132.8, 131.9, 116.1, 113.9, 67.2, 56.4, 36.6, 32.4, 30.5$.

Compound 7

In a dried round-bottomed flask, **9** (1.54 g, 2 mmol) was dissolved in *N,N*-dimethylformamide (30 mL), and then hydroxybenzaldehyde (806 mg, 6.59 mmol) and cesium carbonate (2.15 g, 6.59 mmol) were successively added. The mixture was vigorously stirred and heated at 60 °C for 24 h. The solvent was removed under reduced pressure, the crude residue was dissolved in CH_2Cl_2 (50 mL) and washed with 1 M NaOH solution (50 mL \times 3). The organic phase was dried over anhydrous Na_2SO_4 and concentrated *in vacuo* to give a brown oil. The crude compound was purified by silica gel column chromatography using dichloromethane/ethyl acetate (20:1) as the eluent to give pure **7** as a white solid (1.56 g, 87%). T_m : 105–106 °C. IR: cm^{-1} 3054, 2931, 2831, 2741, 1731, 1680, 1577, 1477, 1453, 1397, 1345, 1251, 1213, 1143, 1110, 1059, 1007, 930, 874, 829, 781, 700, 652, 619, 558. HRMS (ESI): m/z [$\text{M} + \text{Na}$] $^+$ calcd for $\text{C}_{54}\text{H}_{54}\text{O}_{12}$, 971.3507; found at 971.3505; ^1H NMR (400 MHz, CDCl_3) $\delta = 9.86$ (s, 3H), 7.79 (d, $J = 8.8$ Hz, 6H), 6.97 (d, $J = 8.7$ Hz, 6H), 6.87 (s, 3H), 6.80 (s, 3H), 4.73 (d, $J = 13.8$ Hz, 3H), 4.29–4.19 (m, 6H), 4.20–4.10 (m, 6H), 3.75 (s, 9H), 3.51 (d, $J = 13.8$ Hz, 3H), 2.28 (quintuplet, $J = 6.0$ Hz, 6H); ^{13}C NMR (75 MHz, CDCl_3) $\delta = 190.8, 171.2, 163.9, 148.4, 146.9, 132.6, 132.0, 130.0, 115.7, 114.8, 113.9, 65.7, 64.9, 60.4, 56.2, 36.5, 29.2, 21.1, 14.3$.

Compounds 11 and 12

In a two-necked ice-cooled round bottomed flask, **10** (6 g, 32.92 mmol) was dissolved in dry dichloromethane (100 mL), and sulfuryl chloride (2.93 mL, 36.22 mmol) was carefully added drop-wise. The mixture was vigorously stirred under an argon atmosphere at 0 °C and allowed to warm slowly to room temperature for 2 h. The solvent was concentrated *in vacuo* to give compound **11** as a yellow oil (5.45 g, 97%), and directly used in the next step. In a two-necked round bottomed flask, **11** (5 g, 29.31 mmol) was dissolved in dry *N,N*-dimethylformamide (100 mL). Potassium carbonate (6.08 g, 43.97 mmol) and vanillyl alcohol (6.78 g, 43.96 mmol) were then carefully added portion-wise. The mixture was vigorously stirred under an argon atmosphere at room temperature for 36 h. The solvent was then removed under reduced pressure. The residue was dissolved in CH_2Cl_2 (150 mL) and extracted with 1 M NaOH solution (150 mL \times 3) and the organic phase was dried with anhydrous Na_2SO_4 . The solvent was concentrated *in vacuo* to give a brown oil, which was purified by silica gel column chromatography using petroleum ether/ethyl acetate (1:1) to give pure **12** as a white solid (4.31 g, 51%). Compound **12**: T_m : 98–99 °C. IR: cm^{-1} 3402, 2920, 2849, 2744, 1742, 1683, 1598, 1580, 1463, 1420, 1305, 1265, 1208, 1160, 1134, 1082, 1032, 996, 852, 761, 606, 551, 516. HRMS (ESI): m/z [$\text{M} + \text{Na}$] $^+$ calcd for $\text{C}_{16}\text{H}_{16}\text{O}_5$, 311.0890; found at 311.0893; ^1H NMR (300 MHz, CDCl_3) $\delta = 9.90$ (s, 1H), 7.84 (d, $J = 8.8$ Hz, 2H), 7.25 (d, $J = 8.7$ Hz, 2H), 7.07 (d, $J = 8.1$ Hz, 1H), 6.96 (d, $J = 2.0$ Hz, 1H), 6.84 (dd, $J = 8.1, 2.0$ Hz, 1H), 5.78 (s, 2H), 4.62 (d,

$J = 4.0$ Hz, 2H), 3.84 (s, 3H). ^{13}C NMR (101 MHz, CDCl_3) $\delta = 191.1, 162.0, 150.6, 145.1, 137.1, 132.0, 131.3, 119.4, 118.5, 116.7, 111.3, 91.9, 65.2, 56.0$.

Compound 5

In a two-necked round bottomed flask, **12** (4 g, 13.87 mmol) was dissolved in dry dichloromethane (80 mL) and a catalytic amount of scandium(III) triflate (683 mg, 1.39 mmol) was added. The mixture was vigorously stirred under an argon atmosphere and slowly heated at 40 °C for 24 h. The solvent was removed under reduced pressure, the residue was dissolved in CH_2Cl_2 (80 mL) and washed with 1 M NaOH solution (80 mL \times 3) and the organic phase was dried with anhydrous Na_2SO_4 . The solvent was concentrated *in vacuo* to give a brown oil, which was purified by silica gel column chromatography using dichloromethane/ethyl acetate (20:1) to give pure **5** as a white solid (1.58 g, 42%). T_m : 112–113 °C. IR: cm^{-1} 2929, 2871, 2830, 1748, 1607, 1509, 1465, 1443, 1398, 1346, 1320, 1260, 1219, 1193, 1142, 1088, 1011, 942, 876, 851, 775, 701, 622, 570, 548, 509. HRMS (ESI): m/z [$\text{M} + \text{Na}$] $^+$ calcd for $\text{C}_{48}\text{H}_{42}\text{O}_{12}$, 833.2568; found at 833.2566; ^1H NMR (300 MHz, CDCl_3) $\delta = 9.91$ (s, 3H), 7.84 (d, $J = 9.0$ Hz, 6H), 7.22 (d, $J = 9.0$ Hz, 6H), 7.08 (s, 3H), 6.78 (s, 3H), 5.75 (d, $J = 7.2$ Hz, 3H), 5.66 (d, $J = 7.2$ Hz, 3H), 4.71 (d, $J = 13.7$ Hz, 3H), 3.71 (s, 9H), 3.53 (d, $J = 13.8$ Hz, 3H); ^{13}C NMR (75 MHz, CDCl_3) $\delta = 190.9, 162.2, 149.1, 144.6, 135.3, 132.0, 131.9, 131.4, 116.7, 56.1, 36.4$.

Hemicryptophane 2

In a round bottomed flask, a solution of tris(2-aminoethyl) amine (322 μL , 2.14 mmol) dissolved in 200 mL of a 1:1 chloroform/methanol mixture was added to a solution of **5** (1.58 g, 1.95 mmol) in a 1:1 chloroform/methanol mixture (800 mL). The mixture was vigorously stirred at room temperature overnight. Then, the mixture was cooled to 0 °C and sodium borohydride (1.47 g, 38.97 mmol) was carefully added portion-wise. The mixture was stirred and slowly warmed to room temperature for 4 h. After removing the solvent under reduced pressure, the residue was dissolved in CH_2Cl_2 (100 mL) and washed with 1 M NaOH solution (100 mL \times 3) and the organic phase was dried over anhydrous Na_2SO_4 . The solvent was then concentrated *in vacuo* to give a brown oil. The crude compound was purified by silica gel column chromatography using dichloromethane/methanol/triethylamine (10:1:0.1) as the eluent to give the pure cage **2** as a white solid (691 mg, 39%). T_m : 158–160 °C. IR: cm^{-1} 2919, 2829, 1668, 1609, 1587, 1509, 1464, 1446, 1392, 1343, 1263, 1228, 1207, 1140, 1082, 1017, 997, 941, 878, 835, 736, 701, 617, 583. HRMS (ESI): m/z [$\text{M} + 2\text{H}$] $^+$ calcd for $\text{C}_{54}\text{H}_{60}\text{N}_4\text{O}_9$, 455.2253; found at 455.2252; ^1H NMR (400 MHz, CDCl_3) $\delta = 7.19$ (s, 3H), 7.05 (d, $J = 8.6$ Hz, 6H), 6.91 (s, 3H), 6.87 (d, $J = 8.6$ Hz, 6H), 5.83 (d, $J = 7.5$ Hz, 3H), 5.74 (d, $J = 7.5$ Hz, 3H), 4.74 (d, $J = 13.7$ Hz, 3H), 3.84 (s, 9H), 3.61 (s, 6H), 3.56 (d, $J = 13.7$ Hz, 3H), 2.58–2.35 (m, 12H); ^{13}C NMR (101 MHz, CDCl_3) $\delta = 155.8, 147.7, 144.2, 133.2, 131.7, 129.5, 116.8, 115.5, 113.9, 90.2, 56.5, 53.9, 47.6, 36.4$.

Hemicryptophane P-H⁺@2

In an ice-cooled round bottomed flask, bis(dimethylamino)-chlorophosphine (64 μ L, 0.42 mmol) was dissolved in anhydrous dichloromethane (10 mL), the mixture was stirred vigorously under an argon atmosphere at 0 °C for 0.5 h, and then a solution of cage 2 (250 mg, 0.28 mmol) in anhydrous dichloromethane (10 mL) was added. The mixture was stirred and slowly warmed to room temperature, and then heated at 40 °C for 1 day. The solvent was then removed under reduced pressure to give a brown oil, which was purified by silica gel column chromatography using dichloromethane/methanol (10 : 1) as the eluent to give the pure azaphosphatrane P-H⁺@2 as a white solid (238 mg, 89%). T_m : 176–177 °C. IR: cm^{-1} 3367, 2956, 2865, 2112, 1921, 1607, 1508, 1482, 1447, 1392, 1316, 1260, 1204, 1144, 1112, 1083, 1039, 989, 873, 737, 699, 619, 584, 546, 513. HRMS (ESI): m/z [M]⁺ calcd for C₅₄H₅₈N₄O₉P⁺, 937.3936; found at 937.3936; ¹H NMR (300 MHz, CDCl₃) δ = 7.40 (s, 3H), 6.94 (s, 3H), 6.41 (d, J = 8.4 Hz, 6H), 6.18 (d, J = 8.5 Hz, 6H), 5.77 (d, J = 6.5 Hz, 3H), 5.57 (d, J = 6.4 Hz, 3H), 4.83 (d, J = 13.7 Hz, 3H), 4.67 (d, J = 492 Hz, 1H), 3.87–3.70 (m, 3H), 3.64 (d, J = 12.7 Hz, 3H), 3.55 (s, 9H), 3.51–3.18 (m, 12H), 2.94–2.78 (m, 3H); ¹³C NMR (75 MHz, CDCl₃) δ = 155.6, 148.2, 143.9, 134.9, 134.1, 131.7, 129.0, 120.1, 118.7, 113.0, 93.5, 55.4, 53.5, 50.5 (d, J = 13.5 Hz), 47.6 (d, J = 6.7 Hz), 42.5 (d, J = 4.5 Hz), 36.3, 34.7; ³¹P NMR (121 MHz, CDCl₃) δ = –32.3 (d, J = 503 Hz); ³¹P CPD NMR (121 MHz, CDCl₃) δ = –32.16.

Hemicryptophane 4

In a round bottomed flask, a solution of tris(2-aminoethyl) amine (322 μ L, 2.14 mmol) in a 1 : 1 chloroform/methanol mixture (200 mL) was added to a solution of precursor 7 (1.56 g, 1.74 mmol) in 1 : 1 chloroform/methanol (800 mL). The reaction mixture was vigorously stirred at room temperature overnight. Then, sodium borohydride (1.47 g, 38.97 mmol) was carefully added portion-wise at 0 °C, and the mixture was stirred and slowly warmed to room temperature for 4 h. The solvent was removed under reduced pressure and the residue was dissolved in CH₂Cl₂ (100 mL), and washed with 1 M NaOH solution (100 mL \times 3). The organic phase was dried over anhydrous Na₂SO₄ and the solvent was concentrated *in vacuo* to give a brown oil. The crude compound was purified by silica gel column chromatography using dichloromethane/methanol/triethylamine (10 : 1 : 0.1) as the eluent to give pure 4 as a white solid (744 mg, 43%). T_m : 183–184 °C. IR: cm^{-1} 3399, 2932, 1667, 1609, 1583, 1512, 1469, 1397, 1345, 1254, 1220, 1182, 1143, 1086, 1054, 1024, 985, 831, 733, 699, 622, 519. HRMS (ESI): m/z [M + H]⁺ calcd for C₆₀H₇₂N₄O₉, 993.5372; found at 993.5376; ¹H NMR (400 MHz, CD₂Cl₂) δ = 7.07 (d, J = 8.6 Hz, 6H), 6.83 (d, J = 2.4 Hz, 6H), 6.69 (s, 3H), 6.66 (s, 3H), 4.72 (d, J = 13.7 Hz, 3H), 4.20–4.04 (m, 6H), 3.97 (t, J = 6.2 Hz, 6H), 3.77 (s, 9H), 3.51 (t, J = 8.0 Hz, 9H), 2.65–2.58 (m, 6H), 2.58–2.55 (m, 6H), 2.18 (quintuplet d, J = 1.89, 5.6 Hz, 6H); ¹³C NMR (101 MHz, CD₂Cl₂) δ = 158.4, 148.8, 147.7, 132.6, 132.4, 129.3, 115.6, 114.6, 114.5, 65.8, 64.8, 56.8, 48.3, 36.5, 29.6.

Hemicryptophane P-H⁺@4

In an ice-cooled round bottomed flask, bis(dimethylamino)-chlorophosphine (64 μ L, 0.42 mmol) was dissolved in anhydrous dichloromethane (10 mL). The mixture was stirred vigorously under an argon atmosphere at 0 °C for 0.5 h, and then a solution of hemicryptophane 4 (278 mg, 0.28 mmol) in anhydrous dichloromethane (10 mL) was added. The mixture was stirred and slowly warmed to room temperature, and then heated at 40 °C for 1 day. The solvent was then removed under reduced pressure to give a brown oil. The crude compound was purified by silica gel column chromatography using dichloromethane/methanol (10 : 1) as the eluent to give the pure azaphosphatrane P-H⁺@4 as a white solid (249 mg, 84%). T_m : 194–195 °C. IR: cm^{-1} 3398, 2930, 2875, 2432, 1670, 1609, 1584, 1510, 1468, 1396, 1261, 1170, 1144, 1085, 985, 944, 870, 850, 832, 732, 669, 585, 552, 514. HRMS (ESI): m/z [M]⁺ calcd for C₆₀H₇₀N₄O₉P⁺, 1021.4875; found at 1021.4874; ¹H NMR (300 MHz, CD₂Cl₂) δ = 6.88 (d, J = 8.5 Hz, 6H), 6.77 (s, 3H), 6.76 (s, 3H), 6.70 (d, J = 8.5 Hz, 6H), 5.14 (d, J = 501 Hz, 1H), 4.68 (d, J = 13.7 Hz, 3H), 4.16–4.02 (m, 12H), 3.77 (s, 9H), 3.59 (dd, J = 4.9 Hz, 18.8 Hz, 6H), 3.52–3.40 (m, 6H), 3.47 (d, J = 13.7 Hz, 3H), 3.26–3.08 (m, 6H), 2.25–2.14 (m, 6H); ¹³C NMR (75 MHz, CDCl₃) δ = 158.8, 147.7, 147.4, 132.0, 131.5, 129.5, 128.2, 114.7, 114.1, 113.3, 65.9, 64.0, 63.6, 56.6, 36.4, 29.5, 15.4; ³¹P NMR CPD (162 MHz, CDCl₃) δ = –23.72; ³¹P NMR (162 MHz, CDCl₃) δ = –23.77 (d, J = 517 Hz).

Hemicryptophane P@4

Azaphosphatrane P-H⁺@4 (150 mg, 0.14 mmol) was placed in a Schlenk tube and dissolved in anhydrous tetrahydrofuran (3 mL). Then potassium *tert*-butoxide (32 mg, 0.28 mmol) was added carefully. The mixture was stirred under an argon atmosphere at room temperature for 2 h. The solvent was removed *in vacuo* and then anhydrous toluene was added (3 mL). The mixture was stirred at room temperature for an additional 0.5 h, and the precipitate that formed was filtered under argon through a fritted glass. The solvent was removed under vacuum to give the pure proazaphosphatrane P@4 as a light-yellow solid (123 mg, 85%). ¹H NMR (300 MHz, Tol) δ = 7.06 (s, 3H), 7.00 (s, 3H), 6.68 (d, J = 3.0 Hz, 6H), 6.60 (d, J = 8.6 Hz, 6H), 4.58 (d, J = 13.5 Hz, 3H), 3.95–3.73 (m, 12H), 3.64 (dt, J = 6.0 Hz, 9.0 Hz, 3H), 3.58–3.48 (m, 3H), 3.44 (s, 9H), 3.36 (d, J = 13.6 Hz, 3H), 2.91–2.78 (m, 6H), 2.73 (t, J = 5.1 Hz, 6H), 2.00 (ddd, J = 17.6, 9.1, 4.8 Hz, 6H); ¹³C NMR (75 MHz, Tol) δ = 158.5, 149.0, 148.4, 133.6, 132.7, 132.5, 125.6, 115.4, 114.4, 65.2, 64.4, 56.4, 53.9, 53.4, 52.2, 49.3, 36.6, 30.1; ³¹P NMR CPD (121 MHz, Tol) δ = 115.57.

Hemicryptophane 13

In an ice-cooled round bottomed flask, bis(dimethylamino)-chlorophosphine (64 μ L, 0.42 mmol) was dissolved in anhydrous acetonitrile (10 mL). The mixture was stirred vigorously under an argon atmosphere at 0 °C for 0.5 h. Then a solution of hemicryptophane 4 (278 mg, 0.28 mmol) in anhydrous acetonitrile (10 mL) was added. The mixture was stirred and

slowly warmed to room temperature, and then heated at 40 °C for 1 day. The solvent was removed under reduced pressure to give a brown oil. The crude compound was purified by silica gel column chromatography using dichloromethane/methanol (15 : 1) as the eluent to give the pure azaphosphatrane **13** as a white solid (113 mg, 39%). T_m : 198–199 °C. IR: cm^{-1} 3390, 2931, 2400, 1610, 1584, 1512, 1469, 1397, 1347, 1261, 1221, 1180, 1143, 1087, 1054, 1025, 985, 834, 735, 623. HRMS (ESI): m/z $[M]^+$ calcd for $\text{C}_{60}\text{H}_{71}\text{N}_4\text{O}_{10}\text{P}$, 1039.4981; found at 1039.4937; ^1H NMR (400 MHz, CDCl_3) δ = 7.60 (d, J = 8.6 Hz, 2H), 7.11 (d, J = 8.5 Hz, 2H), 6.90 (d, J = 8.5 Hz, 2H), 6.81 (d, J = 3.9 Hz, 2H), 6.79 (s, 2H), 6.76 (s, 3H), 6.74 (d, J = 2.1 Hz, 2H), 6.70 (dd, J = 6.19 Hz, 8.55 Hz, 3H), 4.71 (dd, J = 14.0, 4.4 Hz, 3H), 4.27 (td, J = 3.77 Hz, 9.56 Hz, 2H), 4.22–3.90 (m, 12H), 3.85 (s, 3H), 3.81 (s, 3H), 3.74 (s, 3H), 3.56 (d, J = 13.8 Hz, 3H), 3.53–3.46 (m, 3H), 3.04–2.85 (m, 6H), 2.83–2.42 (m, 6H), 2.37–2.19 (m, 6H); ^{13}C NMR (75 MHz, CDCl_3) δ = 159.3, 158.5, 158.5, 148.1, 147.6, 147.6, 147.5, 147.4, 147.2, 132.5, 132.3, 132.2, 132.1, 131.6, 131.4, 129.6, 128.5, 123.4, 114.9, 114.6, 114.5, 114.5, 114.3, 113.8, 113.3, 113.1, 64.9, 64.5, 56.9, 56.9, 56.6, 45.9, 36.4, 29.4, 29.1, 28.9. ^{31}P NMR CPD (162 MHz, CDCl_3) δ = 15.05.

General procedure for the MBH reaction

para-Substituted benzaldehyde (0.3 mmol) was placed in a 5 mL oven-dried Schlenk tube and dissolved in anhydrous dichloromethane (1 mL). 2-Cyclopenten-1-one or 2-cyclohexen-1-one (0.9 mmol) was added and a solution of P@4 (30 mg, 0.03 mmol) in anhydrous dichloromethane (1 mL) was added drop-wise. The mixture was stirred under an argon atmosphere at room temperature, and a solution of titanium chloride in anhydrous dichloromethane (1 M) (0.3 mL, 0.3 mmol) was then added. The mixture was stirred for 0.5 h and then the reaction was quenched with a saturated aqueous solution of NaHCO_3 (3.0 mL). The mixture was stirred for an additional 0.5 h. The inorganic precipitate was filtered and the organic phase was dried over Na_2SO_4 , filtered, and evaporated under vacuum to give the crude product, which was purified by silica gel column chromatography using petroleum ether/ethyl acetate as the eluent to give the pure compound (Table S1†).

Procedure for the determination of $\text{p}K_a$ of P-H⁺@4 and the determination of kinetics of proton transfer

P-H⁺@4 and compound P@1 were mixed together in CD_3CN . ^1H NMR and ^{13}C NMR spectra were recorded every 20 minutes. The ratio of the concentration of protonated and free base in each compound were calculated thanks to the integration of the different signals for the two species, giving access to the rate constants for protonation and deprotonation. Once the thermodynamic equilibrium was reached, the K_a and $\text{p}K_a$ could be assessed.

- (a) K. Jie, Y. Zhou, E. Li and F. Huang, Nonporous Adaptive Crystals of Pillararenes, *Acc. Chem. Res.*, 2018, **51**, 2064; (b) P. Howlader, E. Zangrando and P. S. Mukherjee, Self-Assembly of Enantiopure Pd_{12} Tetrahedral Homochiral Nanocages with Tetrazole Linkers and Chiral Recognition, *J. Am. Chem. Soc.*, 2020, **142**, 9070; (c) M. Yamashina, Y. Tanaka, R. Lavendomme, T. K. Ronson, M. Pittelkow and J. R. Nitschke, An Antiaromatic-Walled Nanospace, *Nature*, 2019, **574**, 511; (d) S. Akine, M. Miyashita and T. Nabeshima, A Metallo-molecular Cage That Can Close the Apertures with Coordination Bonds, *J. Am. Chem. Soc.*, 2017, **139**, 4631.
- P. A. Gale, J. T. Davis and R. Quesada, Anion transport and supramolecular medicinal chemistry, *Chem. Soc. Rev.*, 2017, **46**, 2497.
- (a) G. Zhang and M. Mastalerz, Organic Cage Compounds – from Shape-Persistency to Function, *Chem. Soc. Rev.*, 2014, **43**, 1934; (b) I. A. Riddell, M. M. J. Smulders, J. K. Clegg and J. R. Nitschke, Encapsulation, Storage and Controlled Release of Sulfur Hexafluoride from a Metal–Organic Capsule, *Chem. Commun.*, 2011, **47**, 457; (c) D. Yang, J. Zhao, Y. Zhao, Y. Lei, L. Cao, X.-J. Yang, M. Davi, N. de Sousa Amadeu, C. Janiak, Z. Zhang, Y.-Y. Wang and B. Wu, Enapsulation of Halocarbons in a Tetrahedral Anion Cage, *Angew. Chem., Int. Ed.*, 2015, **54**, 8658, (*Angew. Chem.*, 2015, **127**, 8782); (d) D. Yang, J. Zhao, L. Yu, X. Lin, W. Zhang, H. Ma, A. Gogoll, Z. Zhang, Y. Wang, X.-J. Yang and B. Wu, Air- and Light-Stable P_4 and As_4 within an Anion-Coordination-Based Tetrahedral Cage, *J. Am. Chem. Soc.*, 2017, **139**, 5946; (e) D. Zhang, T. K. Ronson, W. Wang, L. Xu, H.-B. Yang and J. R. Nitschke, A Cavity-Tailored Metal–Organic Cage Entraps Gases Selectively in Solution and the Amorphous Solid State, *Angew. Chem., Int. Ed.*, 2021, **60**, 11789.
- (a) M. J. Webber and R. Langer, Drug Delivery by Supramolecular Design, *Chem. Soc. Rev.*, 2017, **46**, 6600; (b) X. Ma and Y. Zhao, Biomedical Applications of Supramolecular Systems Based on Host–Guest Interactions, *Chem. Rev.*, 2015, **115**, 7794.
- D. Zhang, T. K. Ronson, R. Lavendomme and J. R. Nitschke, Selective Separation of Polyaromatic Hydrocarbons by Phase Transfer of Coordination Cages, *J. Am. Chem. Soc.*, 2019, **141**, 18949.
- (a) R. Warmuth and M. A. Marvel, 1,2,4,6-Cycloheptatetraene: Room-Temperature Stabilization inside a Hemicarcerand, *Angew. Chem., Int. Ed.*, 2000, **39**, 1117; (b) Y. C. Horng, P. S. Huang, C. C. Hsieh, C. H. Kuo and T. S. Kuo, Selective Encapsulation of Volatile and Reactive

- Methyl Iodide, *Chem. Commun.*, 2012, **48**, 8844; (c) M. Fujita, D. Oguro, M. Miyazawa, H. Oka, K. Yamaguchi and K. Ogura, Self-Assembly of Ten Molecules into Nanometre-Sized Organic Host Frameworks, *Nature*, 1995, **378**, 469; (d) M. Ziegler, J. L. Brumaghim and K. N. Raymond, Stabilization of a Reactive Cationic Species by Supramolecular Encapsulation, *Angew. Chem., Int. Ed.*, 2000, **39**, 4119; (e) S. K. Körner, F. C. Tucci, D. M. Rudkevich, T. Heinz and J. Rebek, A Self-Assembled Cylindrical Capsule: New Supramolecular Phenomena through Encapsulation, *Chem. – Eur. J.*, 2000, **6**, 187; (f) Z. Lin, J. Sun, B. Efremovska and R. Warmuth, Assembly of Water-Soluble, Dynamic, Covalent Container Molecules and Their Application in the Room-Temperature Stabilization of Protoadamantene, *Chem. – Eur. J.*, 2012, **18**, 12864; (g) P. Mal, B. Breiner, K. Rissanen and J. R. Nitschke, White Phosphorus is Air-Stable within a Self-Assembled Tetrahedral Capsule, *Science*, 2009, **324**, 1697.
- 7 (a) M. Yoshizawa, J. K. Klosterman and M. Fujita, Functional Molecular Flasks: New Properties and Reactions within Discrete, Self-Assembled Hosts, *Angew. Chem., Int. Ed.*, 2009, **48**, 3418, (*Angew. Chem.*, 2009, **121**, 3470); (b) S. Zarra, D. M. Wood, D. A. Roberts and J. R. Nitschke, Molecular Containers in Complex Chemical Systems, *Chem. Soc. Rev.*, 2015, **44**, 419; (c) C. J. Brown, F. D. Toste, R. G. Bergman and K. N. Raymond, Supramolecular Catalysis in Metal-Ligand Cluster Hosts, *Chem. Rev.*, 2015, **115**, 3012; (d) Q. Zhang and K. Tiefenbacher, Terpene Cyclization Catalysed inside a Self-Assembled Cavity, *Nat. Chem.*, 2015, **7**, 197; (e) S. H. A. M. Leenders, R. Gramage-Doria, B. de Bruin and J. N. H. Reek, Transition Metal Catalysis in Confined spaces, *Chem. Soc. Rev.*, 2015, **44**, 433; (f) M. Morimoto, S. M. Bierschenk, K. T. Xia, R. G. Bergman, K. N. Raymond and F. Dean Toste, Advances in Supramolecular Host-Mediated Reactivity, *Nat. Catal.*, 2020, **3**, 969; (g) C. Gaeta, P. La Manna, M. De Rosa, A. Soriente, C. Talotta and P. Neri, Supramolecular Catalysis with Self-Assembled Capsules and Cages: What Happens in Confined Spaces, *ChemCatChem*, 2021, **13**, 1638; (h) S. Roland, J. Meijide Suarez and M. Sollogoub, Confinement of Metal-N-Heterocyclic Carbene Complexes to Control Reactivity in Catalytic Reactions, *Chem. – Eur. J.*, 2018, **24**, 12464; (i) D. Matt and J. Harrowfield, Phosphines and other P(III)-derivatives with Cavity-shaped Subunits: Valuable Ligands for Supramolecular Metal Catalysis, Metal Confinement and Subtle Steric Control, *ChemCatChem*, 2021, **13**, 153; (j) G. Olivo, G. Capocasa, D. Del Giudice, O. Lanzalunga and S. Di Stefano, New Horizons for Catalysis Disclosed by Supramolecular Chemistry, *Chem. Soc. Rev.*, 2021, **50**, 7681.
- 8 (a) D. Zhang, T. K. Ronson, Y.-Q. Zou and J. R. Nitschke, Metal–Organic Cages for Molecular Separations, *Nat. Rev. Chem.*, 2021, **5**, 168; (b) S. Pullen, J. Tessarolo and G. H. Clever, Increasing Structural and Functional Complexity in Self-Assembled Coordination Cages, *Chem. Sci.*, 2021, **12**, 7269; (c) M. J. Hardie, Self-assembled Cages and Capsules Using Cyclotrimeratrylene-type Scaffolds, *Chem. Lett.*, 2016, **45**, 1336.
- 9 (a) T. Brotin and J.-P. Dutasta, Cryptophanes and Their Complexes—Present and Future, *Chem. Rev.*, 2009, **109**, 88; (b) H. Xie, T. J. Finnegan, V. W. L. Gunawardana, R. Z. Pavlović, C. E. Moore and J. D. Badjić, A Hexapodal Capsule for the Recognition of Anions, *J. Am. Chem. Soc.*, 2021, **143**, 3874; (c) K. Hermann, Y. Ruan, A. M. Hardin, C. M. Hadad and J. D. Badjić, Gated Molecular Baskets, *Chem. Soc. Rev.*, 2015, **44**, 500; (d) M. Mastalerz, Porous Shape-Persistent Organic Cage Compounds of Different Size, Geometry, and Function, *Acc. Chem. Res.*, 2018, **51**, 2411.
- 10 (a) N.-W. Wu, I. D. Petsalakis, G. Theodorakopoulos, Y. Yu and J. Rebek Jr., Cavitands as Containers for α,ω -Dienes and Chaperones for Olefin Metathesis, *Angew. Chem., Int. Ed.*, 2018, **57**, 15091; (b) H. Takezawa, K. Shitozawa and M. Fujita, Enhanced Reactivity of Twisted Amides inside a Molecular Cage, *Nat. Chem.*, 2020, **12**, 574; (c) D. Masseroni, S. Mosca, M. P. Mower, D. G. Blackmond and J. Rebek, Cavitands as Reaction Vessels and Blocking Groups for Selective Reactions in Water, *Angew. Chem., Int. Ed.*, 2016, **55**, 8290.
- 11 C. M. Hong, M. Morimoto, E. A. Kapustin, N. Alzakhem, R. G. Bergman, K. N. Raymond and F. D. Toste, Deconvoluting the Role of Charge in a Supramolecular Catalyst, *J. Am. Chem. Soc.*, 2018, **140**, 6591.
- 12 (a) Q. Zhang, L. Catti, J. Pleiss and K. Tiefenbacher, Terpene Cyclizations inside a Supramolecular Catalyst: Leaving-Group-Controlled Product Selectivity and Mechanistic Studies, *J. Am. Chem. Soc.*, 2017, **139**, 11482; (b) Q. Zhang, J. Rinkel, B. Goldfuss, J. S. Dickschat and K. Tiefenbacher, Sesquiterpene Cyclisations Catalysed inside the Resorcinarene Capsule and Application in the Short Synthesis of Isolongifolene and Isolongifolenone, *Nat. Catal.*, 2018, **1**, 609; (c) Q. Zhang and K. Tiefenbacher, Sesquiterpene Cyclizations inside the Hexameric Resorcinarene Capsule: Total Synthesis of δ -Selinene and Mechanistic Studies, *Angew. Chem., Int. Ed.*, 2019, **58**, 12688; (d) L.-D. Syntrivanis, I. NémethováL, D. Schmid, S. Levi, A. Prescimone, F. Bissegger, D. T. Major and K. Tiefenbacher, Four-Step Access to the Sesquiterpene Natural Product Presilphiperfolan-1 β -ol and Unnatural Derivatives via Supramolecular Catalysis, *J. Am. Chem. Soc.*, 2020, **142**, 5894.
- 13 (a) S. Giust, G. La Sorella, L. Sporni, G. Strukul and A. Scarso, Substrate Selective Amide Coupling Driven by Encapsulation of a Coupling Agent within a Self-Assembled Hexameric Capsule, *Chem. Commun.*, 2015, **51**, 1658; (b) A. Cavarzan, J. N. H. Reek, F. Trentin, A. Scarso and G. Strukul, Substrate Selectivity in the Alkyne Hydration Mediated by NHC–Au(I) Controlled by Encapsulation of the Catalyst within a Hydrogen Bonded Hexameric Host, *Catal. Sci. Technol.*, 2013, **3**, 2898; (c) L. R. Holloway, P. M. Bogie, Y. Lyon, C. Ngai, T. F. Miller, R. R. Julian and R. J. Hooley,

- Tandem Reactivity of a Self-Assembled Cage Catalyst with Endohedral Acid Groups, *J. Am. Chem. Soc.*, 2018, **140**, 8078; (d) S. S. Nurttala, W. Brenner, J. Mosquera, K. M. van Vliet, J. R. Nitschke and J. N. H. Reek, Size-Selective Hydroformylation by a Rhodium Catalyst Confined in a Supramolecular Cage, *Chem. – Eur. J.*, 2019, **25**, 609; (e) D. Zhang, K. Jamieson, L. Guy, G. Gao, J.-P. Dutasta and A. Martinez, Tailored Oxido-Vanadium(v) Cage Complexes for Selective Sulfoxidation in Confined Spaces, *Chem. Sci.*, 2017, **8**, 789.
- 14 (a) P. Zhang, J. Mejjide Suárez, T. Driant, E. Derat, Y. Zhang, M. Ménand, S. Roland and M. Sollogoub, Cyclodextrin Cavity-Induced Mechanistic Switch in Copper-Catalyzed Hydroboration, *Angew. Chem., Int. Ed.*, 2017, **56**, 10821; (b) M. Guitet, P. Zhang, F. Marcelo, C. Tugny, J. Jiménez-Barbero, O. Buriez, C. Amatore, V. Mourières-Mansuy, J.-P. Goddard, L. Fensterbank, Y. Zhang, S. Roland, M. Mealand and M. Sollogoub, NHC-Capped Cyclodextrins (ICyDs): Insulated Metal Complexes, Commutable Multicoordination Sphere, and Cavity-Dependent Catalysis, *Angew. Chem., Int. Ed.*, 2013, **52**, 7213.
- 15 H. Takezawa, T. Kanda, H. Nanjo and M. Fujita, Site-Selective Functionalization of Linear Diterpenoids through U-Shaped Folding in a Confined Artificial Cavity, *J. Am. Chem. Soc.*, 2019, **141**, 5112.
- 16 (a) H. Takezawa, T. Kanda, H. Nanjo and M. Fujita, Site-Selective Functionalization of Linear Diterpenoids through U-Shaped Folding in a Confined Artificial Cavity, *J. Am. Chem. Soc.*, 2019, **141**, 5112; (b) C. Fuertes-Espinosa, C. Garcia-Simón, M. Pujals, M. Garcia-Borras, L. Gomez, T. Parella, J. Juanhuix, I. Imaz, D. MasPOCH, M. Costas and X. Ribas, Supramolecular Fullerene Sponges As Catalytic Masks for Regioselective Functionalization of C60, *Chem*, 2020, **16**, 169; (c) E. Ubasart, O. Borodin, C. Fuertes-Espinosa, Y. Xu, C. García-Simón, L. Gómez, J. Juanhuix, F. Gándara, I. Imaz, D. MasPOCH, M. von Delius and X. Ribas, A Three-Shell Supramolecular Complex Enables the Symmetry-Mismatched Chemo- and Regioselective Bis-Functionalization of C60, *Nat. Chem.*, 2021, **13**, 420.
- 17 Y. Ueda, H. Ito, D. Fujita and M. Fujita, Permeable Self-Assembled Molecular Containers for Catalyst Isolation Enabling Two-Step Cascade Reactions, *J. Am. Chem. Soc.*, 2017, **139**, 6090.
- 18 J. Yang, B. Chatelet, V. Dufaud, D. Héroult, S. Michaud-Chevallier, V. Robert, J.-P. Dutasta and A. Martinez, Endohedral Functionalized Cage as a Tool to Create Frustrated Lewis Pairs, *Angew. Chem., Int. Ed.*, 2018, **57**, 14212.
- 19 (a) D. W. Stephan, Frustrated Lewis Pairs: From Concept to Catalysis, *Acc. Chem. Res.*, 2015, **48**, 306; (b) D. W. Stephan and G. Erker, Frustrated Lewis Pair Chemistry: development and perspectives, *Angew. Chem., Int. Ed.*, 2015, **54**, 6400; (c) D. W. Stephan, Frustrated Lewis Pairs, *J. Am. Chem. Soc.*, 2015, **137**, 10018; (d) D. W. Stephan and G. Erker, Frustrated Lewis Pairs: Metal-Free Hydrogen Activation and more, *Angew. Chem., Int. Ed.*, 2010, **49**, 46-76; (e) D. W. Stephan, The Broadening Reach of Frustrated Lewis Pair Chemistry, *Science*, 2016, **354**, 6317; (f) G. Kehr and G. Erker, Frustrated Lewis Pair Chemistry: Searching for New Reaction, *Chem. Rec.*, 2017, **17**, 803.
- 20 (a) A. I. Briceno-Strocchia, T. C. Johnstone and D. W. Stephan, Using Frustrated Lewis Pairs to Explore C-F bond Activation, *Dalton Trans.*, 2020, **49**, 1319; (b) M. A. Légaré, M. Courtemanche, E. Rochette and F. G. Fontaine, Boron catalysis. Metal-Free Catalytic C-H Bond Activation and Borylation of Heteroarenes, *Science*, 2015, **349**, 513; (c) A. Brar, S. Mummadi, D. K. Unruh and C. Krempner, “Inverse” Frustrated Lewis Pairs: An Inverse FLP Approach to the Catalytic Metal Free Hydrogenation of Ketones, *Organometallics*, 2020, **39**, 4307.
- 21 (a) J. Lam, K. M. Szkop, E. Mosaferi and D. W. Stephan, FLP Catalysis: Main Group Hydrogenations of Organic Unsaturated Substrates, *Chem. Soc. Rev.*, 2019, **48**, 3592; (b) A. Simonneau, R. Turrel, L. Vendier and M. Etienne, Group 6 Transition-Metal/Boron Frustrated Lewis Pair Templates Activate N₂ and Allow its Facile Borylation and Silylation, *Angew. Chem., Int. Ed.*, 2017, **56**, 12268; (c) N. Von Wolff, G. Lefèvre, J.-C. Berthet, P. Thuéry and T. Cantat, Implications of CO₂ Activation by Frustrated Lewis Pairs in the Catalytic Hydroboration of CO₂: A View Using N/Si⁺ Frustrated Lewis Pairs, *ACS Catal.*, 2016, **6**, 4526.
- 22 D. W. Stephan, Catalysis, FLPs, and Beyond, *Chem*, 2020, **6**, 1520.
- 23 (a) N. Hidalgo, J. J. Moreno, M. Pérez-Jiménez, C. Maya, J. López-Serrano and J. Campos, Tuning Activity and Selectivity during Alkyne Activation by Gold(I)/Platinum(0) Frustrated Lewis Pairs, *Organometallics*, 2020, **39**, 2534; (b) Q. Liu, L. Yang, C. Yao, J. Geng, Y. Wu and Xi. Hu, Controlling the Lewis Acidity and Polymerizing Effectively Prevent Frustrated Lewis Pairs from Deactivation in the Hydrogenation of Terminal Alkynes, *Org. Lett.*, 2021, **23**, 3685; (c) C. Rosorius, G. Kehr, R. Fröhlich, S. Grimme and G. Erker, Electronic Control of Frustrated Lewis Pair Behavior: Chemistry of a Geminal Alkylidene-Bridged Per-pentafluorophenylated P/B Pair, *Organometallics*, 2011, **30**, 4211.
- 24 J. Backs, M. Lange, J. Possart, A. Wollschlger, C. Mgck-Lichtenfeld and W. Uhl, Facile Modulation of FLP Properties: A Phosphinylvinyl Grignard Reagent and Ga/P- and In/P2-Based Frustrated Lewis Pairs, *Angew. Chem., Int. Ed.*, 2017, **56**, 3094.
- 25 (a) S. Mummadi, D. K. Unruh, J. Zhao, S. Li and C. Krempner, “Inverse” Frustrated Lewis Pairs—activation of Dihydrogen with Organosuperbases and Moderate to Weak Lewis Acids, *J. Am. Chem. Soc.*, 2016, **138**, 3286; (b) S. Mummadi, D. Kenefake, R. Diaz, D. K. Unruh and C. Krempner, Interactions of Verkade’s Superbase with Strong Lewis Acids: From Labile Mono- and Binuclear Lewis Acid-Base Complexes to Phosphenium Cations, *Inorg. Chem.*, 2017, **56**, 10748; (c) C. Manankandayalage, D. K. Unruh and C. Krempner, Small Molecule Activation

- with Intramolecular "Inverse" Frustrated Lewis Pairs, *Chem. – Eur. J.*, 2021, **27**, 6263.
- 26 (a) G. Verkade and P. Kisanga, Proazaphosphatranes: a Synthesis Methodology Trip from their Discovery to Vitamin A, *Tetrahedron*, 2003, **59**, 7819; (b) P. Kisanga, J. G. Verkade and R. J. Schwesinger, pKa Measurements of P(RNCH₂CH₂)₃N, *J. Org. Chem.*, 2000, **65**, 5431; (c) M. A. H. Laramay and J. G. Verkade, The "Anomalous" Basicity of P(NHCH₂CH₂)₃N Relative to P(NMeCH₂CH₂)₃N and P(NBzCH₂CH₂)₃N: a Chemical Consequence of Orbital Charge Balance?, *J. Am. Chem. Soc.*, 1990, **112**, 9421.
- 27 B. Chatelet, E. Payet, O. Perraud, P. Dimitrov-Raytchev, L.-C. Chapellet, V. Dufaud, A. Martinez and J.-P. Dutasta, Shorter and Modular Synthesis of Hemicryptophane-tren Derivatives, *Org. Lett.*, 2011, **13**, 3706.
- 28 (a) P. Dimitrov Raytchev, A. Martinez, H. Gornitzka and J.-P. Dutasta, Encaging the Verkade's Superbases: Thermodynamic and Kinetic Consequences, *J. Am. Chem. Soc.*, 2011, **133**, 2157; (b) B. Chatelet, H. Gornitzka, V. Dufaud, E. Jeanneau, J.-P. Dutasta and A. Martinez, Superbases in Confined Space: Control of the Basicity and Reactivity of the Proton Transfer, *J. Am. Chem. Soc.*, 2013, **135**, 18659.
- 29 G. Qiu, P. Nava, C. Colomban and A. Martinez, Control and Transfer of Chirality Within Well-Defined Tripodal Supramolecular Cages, *Front. Chem.*, 2020, **8**, 994.
- 30 H. Achenbach and J. Witzke, Joachim, Untersuchungen an natürlichen γ - und δ -Lactonen, XI. Synthese von Psilotin und 6-Epipsilotin, *Liebigs Ann. Chem.*, 1981, **12**, 2384.